

Cyclic analysis of RC frames with respect to employing different methods in the fiber model for consideration of bond-slip effect

Seyed Shaker HASHEMI*, Mohammad VAGHEFI

Civil Engineering Department, Persian Gulf University, Bushehr-IRAN

e-mail: sh.hashemi@pgu.ac.ir

Received: 14.12.2010

Abstract

In this research, based on a nonlinear analysis of reinforced concrete moment-resisting frames, the bond-slip effect between concrete and bars along the lengths of beam, column, and joint elements was applied to numerical equations. The governing theory in the numerical equations was similar to that of the fiber model, but the perfect bond assumption between the concrete and bar was removed. The precision of the proposed method in considering the real nonlinear behavior of reinforced concrete frames was compared to the precision of other suggested methods for considering the bond-slip effect in fiber model analysis. Among the capabilities of this method are its ability of modeling the embedded lengths of bars within joints and nonlinear modeling of bond-slip. The precision of the analytical results were compared with the experimental results achieved from 2 specimens under cyclic loading. The comparison showed that the proposed method can model the nonlinear behavior of reinforced concrete frames with very good precision.

Key Words: Bond-slip effect, pull-out effect, cyclic analysis, RC frames

1. Introduction

Many analytical models have been devised for the nonlinear analysis of reinforced concrete (RC) frames. Although 2-dimensional and 3-dimensional modeling in a finite element method can make for more accurate analysis, it considerably increases the expense and time of analysis. Therefore, such methods are typically used for modeling structural parts while easier methods are utilized for the full modeling of structures. The one-component model of Clough et al. (1965) is one of the simple models used for nonlinear analysis of RC frames. Various models with concentrated plasticity (Brancaleoni et al., 1983) were presented later and a more accurate description of the nonlinear behavior of the elements of RC frames became available through models with distributed plasticity (Soleimani et al., 1979). Other models (Filippou et al., 1992), including multispring models that use subelements, were devised. One of the most commonly used methods is the fiber model. In this method, an element is divided into a number of concrete and steel fiber lengths, and the element section specifications are worked out by adding up the effects of the fibers' behavior. This method assumes a perfect bond between concrete and bar (Spacone et al., 1996; Mazars et al, 2006), but this assumption is not very

*Corresponding author

appropriate or realistic and causes a considerable difference between analytical and experimental results (Kwak and Kim, 2006). Belarbi and Hsu (1994), as well as Kwak and Kim (2002), made use of the fiber method, but in order to modify it and reduce the error of analysis resulting from the perfect bond assumption, they modified the stress-strain behavior of the bars. In this way, they drew on an equivalent method. Limkatanyu and Spacone (2002a) used the fiber model but removed the perfect bond assumption. In order to achieve this, they differentiated between the degrees of freedom of the concrete and of the bars in the beam-column elements. This modified method was used for beam-column elements in the present study, but for modeling RC frames, a joint element is also needed. What matters is the compatibility and assimilability of joint elements with beam-column elements. In initial methods of nonlinear analysis of RC frames, the nonlinear effect of beam-column joints is considered using calibration of plastic hinges within adjacent beam-column elements (Otani, 1974). In such a situation, the joint element is not modeled separately, but rather its effect on the adjacent elements is considered. From there, the joints of RC frames are located in critical zones and they are affected by different effects such as high shear force and the bond-slip effect, so the joints need more precise modeling (Lee et al., 2009). Based on another approach, the behaviors of each of the elements of joint, beam, and column are separated. The zero-length rotational spring is one such joint element (Alath and Kunnath, 1995). In this kind of modeling, the effect of shear deformation is considered using a spring whose governing behavior is moment-rotation. In another type, as in the previous approach, 2 springs are used in the joint modeling. In one spring, the effect of shear deformation is taken into account, and in the other, the effect of deformation resulting from bar slip is taken into account (Biddah and Ghobarah, 1999). In order to calibrate such joint elements, experimental results or estimated force-deformation relationships at the joints should be used, but a precise calculation of such relationships is not easy, especially in structures that enjoy a high multiplicity of joint element types. Moreover, in such cases, various factors affecting the nonlinear behavior of joints are not separated but are generally applied in the models. In some newer methods, joint elements are modeled as 2-dimensional planes, but in order to use such elements along with adjacent beam-column elements in assembling the whole of the RC frame, transient elements are also utilized so that there will be a connection between the degrees of freedom of joint plane and of adjacent linear elements (Elmorsi et al., 2000). Such elements typically have 2-dimensional formulations and are capable of separately modeling the behavior of concrete and bars and the interactions between them. These elements, however, like finite element methods, increase the modeling time and the amount of calculations. Furthermore, when there is a need for the degrees of freedom of the concrete and bars in the joint element to be compatible with the corresponding degrees of freedom in the adjacent linear beam-column elements, this type of modeling has its own limitations. Another type of joint element is created by assembling a series of one-dimensional components that are used for modeling the dominant behavior of joint elements and whose calibration is carried out through experimental results (Lowe et al., 2004). This kind of modeling relies on the behavior of force deformation for each effective component, and because force-deformation relations are calculated approximately, such modeling will not be completely precise and will need a strong calibration process. Limkatanyu (2000) introduced an interior joint element based on the separation of the degrees of freedom of bars going through the joints and concrete. Although this element can model the interaction between concrete and bars very well, it loses precision because it presupposes identical degrees of freedom for all 4 sides around the joint element and ignores the shear deformation of joint planes. Another important point about the existing types of models is that most of them cannot be used for studying joints in different frame locations. Thus, most of them are useful for only one of various interior, exterior, or corner locations.

In the present study, the beam-column element introduced by Limkatanyu and Spacone (2002a) was used for modeling beam and column elements since it enjoys good precision and includes the interaction between the concrete and bars (Limkatanyu and Spacone, 2002b). A joint element was also defined and used, which, in addition to its flexibility in modeling different types of joint elements such as interior, exterior, corner, and footing, is capable of being assembled with the above beam-column element. Moreover, this modeling takes into consideration such factors as the bond-slip effect between the bars that pass through joints, the pull-out effect of bars that are restrained within joints, the nonlinear behavior of materials, and the shear-deformation effect of different beam-column elements. The introduced modeling is easy to use. In order to model the joint elements, a pull-out mechanism, an RC subelement, and a concrete subelement were first defined as the composing parts of the RC joint element. These parts were then assembled to produce 4 types of joint elements to be used along with beam-column elements in the modeling of RC moment-resisting frames. For simplicity's sake, RCF, RCMRF, BCE, JE, RCSE, and CSE are used in the text instead of reinforced concrete frame, reinforced concrete moment-resisting frame, beam-column element, joint element, reinforced concrete subelement, and concrete subelement, respectively.

2. Nonlinear analysis of RCF

For the purpose of nonlinear analysis of RCFs and evaluation of the proposed method, 4 kinds of analyses were examined, as shown in Table 1. In order to carry out the investigations, a computer program created in MATLAB software was used by the authors (MathWorks, 2008).

Table 1. Details of analyses 1-4.

Analysis	Description	Nonlinear modeling specifications				
		Modeling of BCE	Modeling of JE	Applying bond-slip effect in calculations		Applying pull-out effect in calculations
				Indirectly as an equivalent method	Directly	
1	Nonlinear analysis using fiber model with perfect bond assumption	Yes	No	No	No	No
2	Nonlinear analysis using fiber model and applying bond-slip effect by modifying the yielding point in stress-strain behavior of the bars	Yes	No	Yes	No	No
3	Nonlinear analysis using the fiber model and applying bond-slip effect by modifying the yielding point and elasticity modulus in the stress-strain behavior of the bars	Yes	No	Yes	No	No
4	Nonlinear analysis using proposed method from this study	Yes	Yes	No	Yes	Yes

2.1. Slip effect in reinforced concrete

The bond effect is an important factor in explaining local failures as well as the rates of energy absorption and of waste of the components of the inner force in RC members. A reduction in bond stress leads to the redistribution of internal forces. When, under the effect of applied forces, a crack in an RC member is created (Figure 1), cracks appear along with strain ε_{S2} on both sides of the member. On parts further from the crack

faces, the axial force of the bar is transferred to the concrete with the help of the bond stress. The value of the bond stress is zero in the inner parts of the transfer length (l_t), and it is maximum on the crack faces. This means that there is no slip in the middle or central parts, which cover the distance between the 2 transfer lengths on the 2 sides ($L - 2l_t$) (Kwak and Song, 2006).

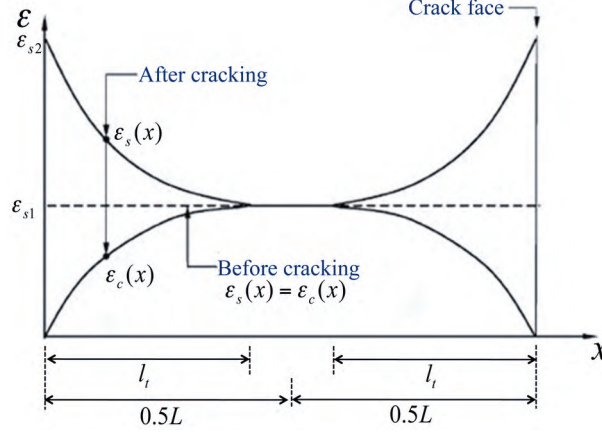


Figure 1. Strain distribution in cracked reinforced concrete (Kwak and Song, 2006).

It is assumed that after the occurrence of a crack, the strain values of the concrete and bar are the same at point $x = l_t$ and are both ε_{s1} . Based on the distribution of the strain, we may calculate the local slip by evaluating the difference between length variations of the bar and concrete at distance x from the crack face and the middle point of the cracked member ($x = L/2$), as shown in Eq. (1) (Kwak and Kim, 2006).

$$s(x) = \int_x^{L/2} (\varepsilon_s(x) - \varepsilon_c(x)) dx \quad (1)$$

In the above equation, L is the length of the distance between neighboring cracks, which is called the crack space. $\varepsilon_s(x)$ and $\varepsilon_c(x)$ are the bar and concrete strain distributions, respectively. Considering the bond effect and the free body diagram of a length segment between the 2 cracks, and assuming the linearity of the equation of bond stress and slip as $\tau_b = E_b * s(x)$, the function of slip distribution $s(x)$ will be obtained in the form of Eq. (2).

$$\frac{d^2 s(x)}{dx^2} - k^2 s(x) = 0, \quad k^2 = m \sum_0 E_b (1 + n\rho) / A_s E_s, \quad n = \frac{E_s}{E_c}, \quad \rho = \frac{A_s}{A_c} \quad (2)$$

E_b is the slip modulus and is assumed to be $1.826 \times 10^4 \text{ MN}/\text{m}^3$ by Kwak and Kim (2006). m is the number of tensile bars and \sum_0 is the circumference of a bar section. The general answer to differential Eq. (2) will be in the form of Eq. (3).

$$s(x) = C_1 \sinh(x) + C_2 \cosh(x) \quad (3)$$

In the above equation, the C_1 and C_2 constants are calculated from boundary conditions. In the boundary conditions, the slip at $x = l_t$ is zero, and at $x = 0$, which is the crack face, it is maximum (S_0). It can be assumed that the crack width is twice as much as the maximum of S_0 ($S_0 = w/2$) (Kwak and Kim, 2006). Researchers have proposed some equations for calculating crack widths (Piyasena, 2002). For calculating the

transient length, experimental or analytical equations can be used based on the equivalent force of the RC element between the 2 cracks. After obtaining the specifications of the bond along the length of the member, we can evaluate the slip and stress distributions of the distance between 2 neighboring cracks.

2.2. Description of analysis 1

In this type of analysis, which is a nonlinear analysis using the fiber model, the JE is not modeled. Formulation of each RC beam or column element is done based on the Euler-Bernoulli beam theory. The cross-section of the RC BCE is divided into a suitable number of concrete and steel fibers (bars). As shown in Figure 2, the value of the length strain corresponding to each concrete or steel fiber is calculated with regard to its position in the cross-section assuming a linear distribution of strain in the section of the RC element. This means that the possible slip effect of the longitudinal bar is ignored, since if the bar slips, the value of the longitudinal strain of the bar will not be the same as the value obtained through the above method. This is the main assumption in the fiber model and it is referred to as the perfect bond assumption.

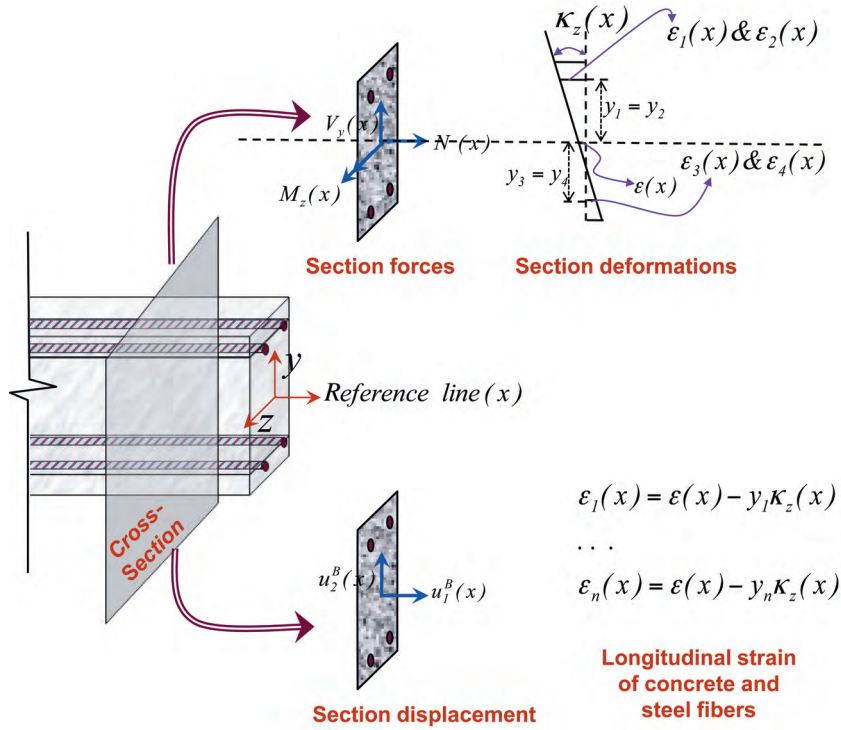


Figure 2. Specifications of element section in the theory of fiber model.

2.3. Description of analysis 2

This analysis is very similar to analysis 1 and is in fact a fiber model, but for the purpose of reducing errors induced by the perfect bond assumption, the analysis is modified into an equivalent yielding point in the bar stress-strain diagram of a nonlinear solution. If the yielding point stress of the bar obtained from tensile tests without concrete is σ_y , the yielding point of the bars will be assumed to be lower than σ_y and used in numerical calculations. This is because yielding occurs in an RC member when a bar in the cracked section reaches the yielding point of the bare bar, whereas the average stress of the bar in the cracked member is elastic and less

than the yielding point. This happens because the bar is surrounded by concrete, and the concrete between the 2 cracks can bear the pulling forces due to the bond between the concrete and bar. Based on this theory and research done by Belarbi and Hsu (1994), the bar stress-strain equation is modified into Eq. (4) (Figure 3).

$$\begin{cases} \sigma_s = E_s \cdot \varepsilon_s & : \varepsilon_s \leq \varepsilon_n \\ \sigma_s = \sigma_n + (0.02 + 0.25B_B)E_s(\varepsilon_s - \varepsilon_n), B_B = (f_t/\sigma_y)^{1.5}/\rho, \varepsilon_n = \varepsilon_y(0.93 - 2B_B) & : \varepsilon_s \geq \varepsilon_n \end{cases} \quad (4)$$

In the above equations, ε_s and σ_s are the bar strain and stress, respectively. ε_y and σ_y are the bare bar yielding point strain and stress, respectively, and f_t is the tensile strength of the concrete. ρ is the ratio of the bar cross-sectional area to the cross-sectional area of the whole RC section, which must be more than 0.005.

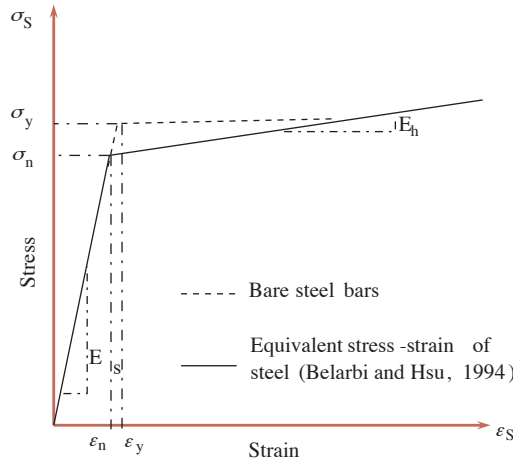


Figure 3. Modification of stress-strain relation of steel bars in analysis 2.

2.4. Description of analysis 3

For the purpose of reducing errors induced from the perfect bond assumption, in this type of analysis, as in analysis 2, the yield stress of the bar is modified into an equivalent value in the nonlinear solution. Here, however, not only the yielding point but also the bar elasticity modulus is modified.

In this type of analysis, based on the function of slip distribution between cracks in Eq. (3) and assuming a linear relationship between slip and bond stress, the axial force balance of a concrete length segment and of adjacent bars is studied. The axial force (N) is appropriately divided between the bar and the adjacent concrete, thereby creating a balance. The stress in the concrete and the bar is calculated using their axial force. In a length equal to half of the distance between the 2 cracks, the function of the bar stress and strain distributions, $\varepsilon_S(x)$ and $\sigma_S(x)$, is similar to that shown in Figure 4a. Assuming a perfect bar-concrete bond and ignoring slip in the fiber model, the stress in the bar must remain unchanged. This means that the equivalent stress in the bar (σ_{eq}^s) and in the transient length (l_t) must be equal to the bar stress outside this area (σ_0^s). Thus, Eq. (5) must be satisfied. In this way, the equivalent modulus of elasticity can be calculated using Eq. (6) (Figure 4b). For more information regarding the numerical calculation of the equivalent elasticity modulus and use of this calculation in fiber model analyses, see the work of Kwak and Kim (2006). In this analysis, the value of the bar's yielding point stress is reduced, as in analysis 2. Figure 5 shows a comparison of the method of reducing

the yielding point in analysis 2 and the method of reducing the elasticity modulus along with the yielding point in analysis 3.

$$\sigma_{eq}^s = E_{eq} \varepsilon_{eq}^s \equiv \sigma_0^s = E_s \varepsilon_{s1} \quad (5)$$

$$E_{eq} = E_s \varepsilon_{s1} / \varepsilon_{eq}^s, \quad E_{eq-h} = E_h \varepsilon_{s1} / \varepsilon_{eq}^s \quad (6)$$

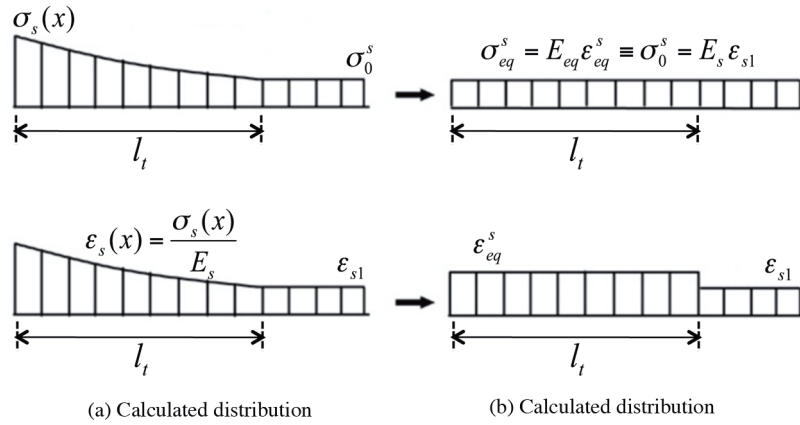


Figure 4. Distribution of slip and stresses between 2 adjacent cracks (Kwak and Kim, 2006).

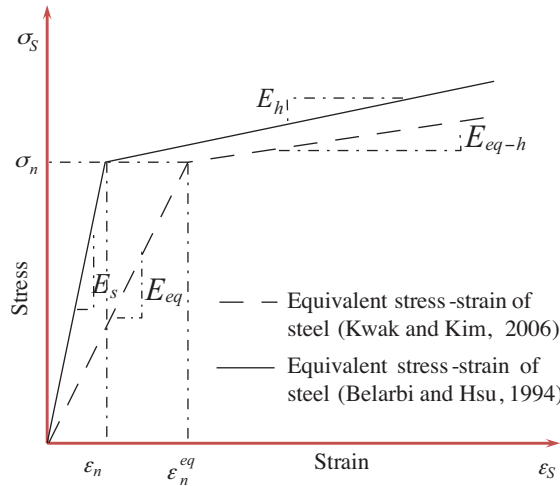


Figure 5. Comparison of equivalent stress-strain relation of analyses 2 and 3.

2.5. Description of analysis 4

In this type of analysis, both the BCE and the JE are modeled. As shown in Figure 6, depending on the position of the joint in the RCF, 4 types of joints can be defined.

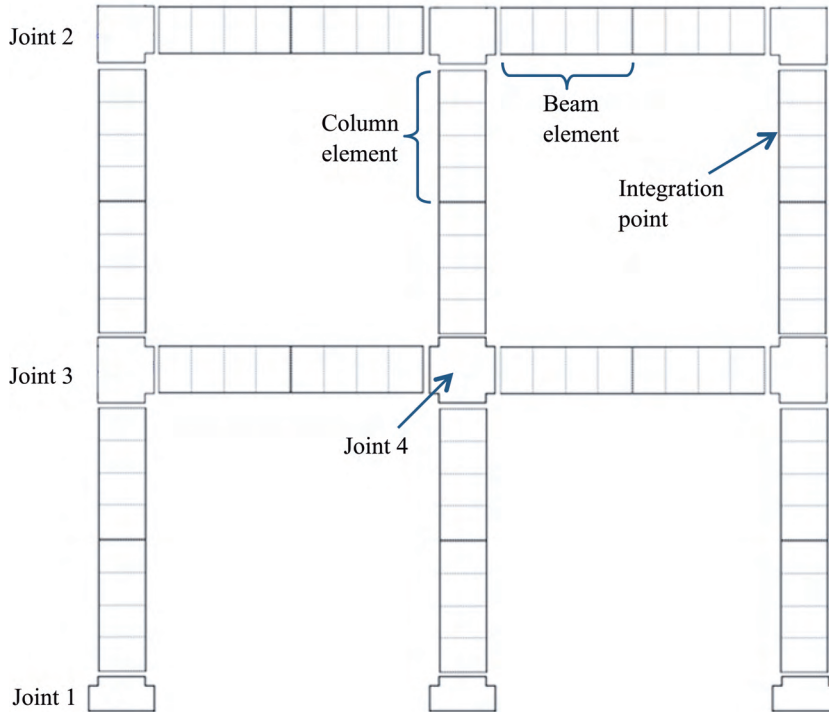


Figure 6. Modeling of RCMRF with BCEs and several types of JEs.

2.5.1. Modeling of BCE

For modeling a BCE based on research carried out by Limkatanyu and Spacone (2002a), in the fiber model, the slip effect between concrete and bar is implemented without ignoring the compatibility of the strain between the concrete and bar. In this method, a length segment of an RCF element is considered as a combination of a length segment of a 2-node concrete element and a number of steel bar elements (i.e., longitudinal bars). The 2-node concrete elements follow the Euler-Bernoulli theory, and the 2-node bar elements are in fact truss elements. Contact between concrete and longitudinal bars is provided by a constant bond force around the bars. Using the internal force balance equations as well as the concrete element axial force equations, steel bar element equations, shear force balance, and flexural force balance in the length segment, the governing equations of the length segment of the BCE are obtained. A weak form of the governing equation in the finite element method is obtained using the shape functions based on displacement and using the principle of stationary potential energy. In this way, in addition to considering the bond-slip effect, using this element will become possible in the modeling of RCFs. Since the degrees of freedom attributed to the concrete element and bars are different, the degrees of freedom of this element, compared to those of other one-dimensional elements used in the modeling of RCFs, are higher and change according to the number of longitudinal bars. It can be argued that this element is ultimately made up of a 2-node beam concrete element and n number of 2-node bar elements (longitudinal bars) along with the bond effect between them. More information on this element can be found in the work of Limkatanyu and Spacone (2002a) (Figure 7).

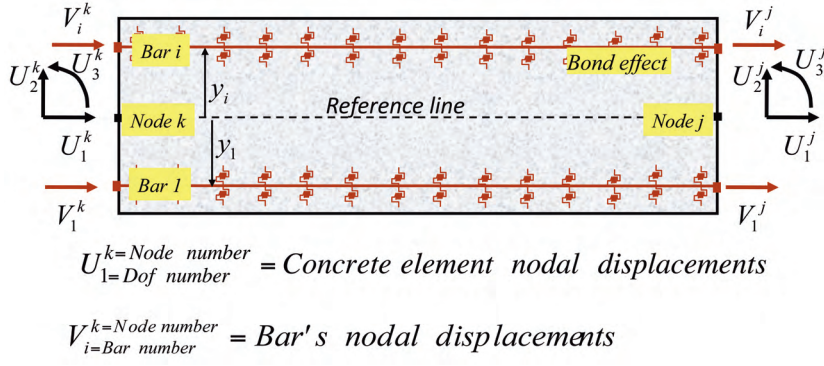


Figure 7. Reinforced concrete BCE.

2.5.2. Modeling of JEs

As shown in Figure 6, 4 types of elements are needed for modeling a JE. For the sake of simplicity in modeling, 2 subelements and a mechanism are first defined, including an RCSE, a CSE, and a bar pull-out mechanism. The different types of JE are then made by assembling the subelements and the mechanism.

Referring to Figure 8, in the pull-out mechanism, the slippage of the bars can be defined in the form of Eq.

(7) if the nodal displacement vector related to pull-out behavior is defined as $\mathbf{U}_{PO} = [U_1^1 \ U_2^1 \ U_3^1 \ V_1^1 \ \dots \ V_n^1]$

$$\mathbf{PO} = \begin{bmatrix} d_{b_1} \\ d_{b_2} \\ \vdots \\ d_{b_n} \end{bmatrix} = \begin{bmatrix} -1 & 0 & y_1 & 1 & 0 & \dots & 0 \\ -1 & 0 & y_2 & 0 & 1 & \dots & 0 \\ \vdots & \vdots & \vdots & \vdots & \vdots & \vdots & \vdots \\ -1 & 0 & y_n & 0 & 0 & \dots & 1 \end{bmatrix} \mathbf{U}_{PO} = \mathbf{A}_{PO} \mathbf{U}_{PO} \quad (7)$$

In this equation, y_n is the distance of the n^{th} bar from the reference line. The relationship between the pull-out force and slip for the embedded n^{th} bar in the section can be defined as $f_{PO_n} = k_{PO_n} \times d_{b_n}$, in which f_{PO_n} is the pull-out force and k_{PO_n} is the slip stiffness of the pull-out behavior. This equation derives from the bond stress-slip relationship related to the pull-out behavior, embedded length of the bar, condition at the end of the bar, and circumference of the bar cross-section. The relationship between the pull-out force and slip of all bars in the section can be written in the following matrix form:

$$\mathbf{f}_{PO} = \mathbf{k}_{PO} \times \mathbf{PO}, \quad (8)$$

where \mathbf{k}_{PO} is a diagonal matrix that includes k_{PO_n} and \mathbf{f}_{PO} is the pull-out force vector according to the \mathbf{PO} vector.

The nodal force vector can be expressed in the following form:

$$\mathbf{F}_{PO} = \mathbf{A}_{PO}^T \mathbf{f}_{PO} = \mathbf{A}_{PO}^T \mathbf{k}_{PO} \mathbf{PO} = \mathbf{A}_{PO}^T \mathbf{k}_{PO} \mathbf{A}_{PO} \mathbf{U}_{PO} = \mathbf{K}_{PO} \mathbf{U}_{PO}. \quad (9)$$

From Eq. (9), the pull-out stiffness matrix related to the section can be written as $\mathbf{A}_{PO}^T \mathbf{k}_{PO} \mathbf{A}_{PO}$. The pull-out stiffness matrix will be put into the stiffness matrix of the JE. In order to calculate the resisting force vector related to the pull-out behavior and put it into the resisting force vector of the JE, it can be written in the form of $\mathbf{A}_{PO}^T \mathbf{f}_{PO}$.

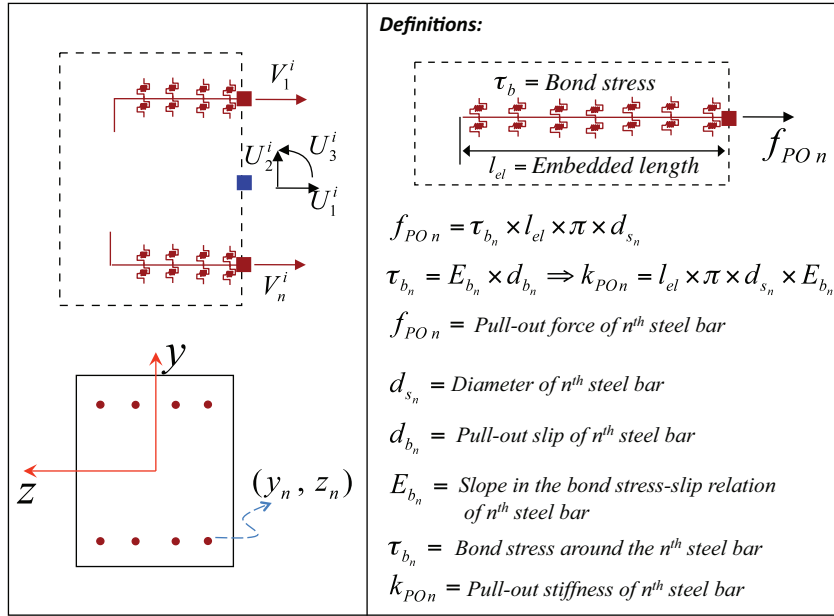


Figure 8. Modeling of pull-out mechanism.

The RCSE is shown in Figure 9. This subelement was produced based on a segment length similar to that of BCE, but it follows the Timoshenko beam theory. This subelement is capable of considering shear deformation and bond-slip effects in nonlinear behavior. As shown in Figure 9, the subelement is affected by 2 distributed external forces: $p_{y1}(x)$ and $p_{y2}(x)$. Since the subelement is part of the JE, the external forces are considered as boundary conditions and obtained in nonlinear solution schemes through the internal forces of the 2 sides of the element; they are continually updated.

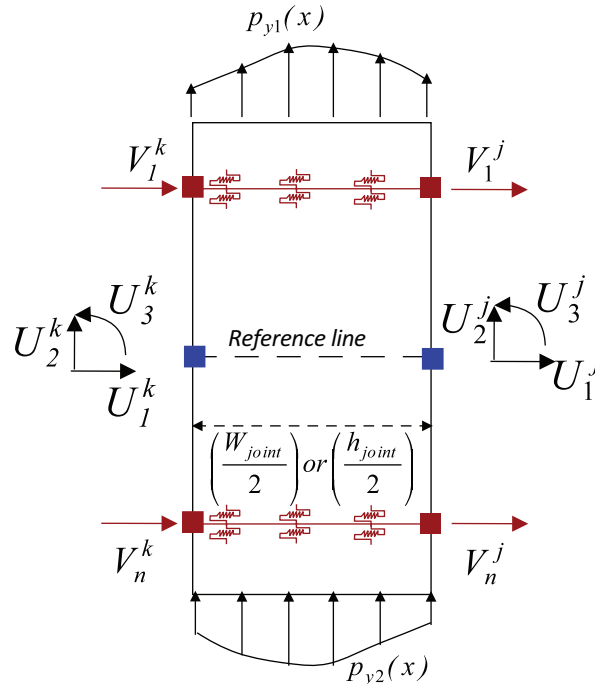


Figure 9. Reinforced concrete subelement.

The CSE is in fact a 2-node concrete element that follows the Timoshenko beam theory and thus considers shear deformation. The CSE, like the RCSE, has boundary conditions in the form of a distributed external force. More details on the formulation of RCSEs and CSEs can be found in the work of Hashemi et al. (2009). Different types of JEs, as shown in Figure 10, are modeled by assembling the subelements and the bar's pull-out mechanism.

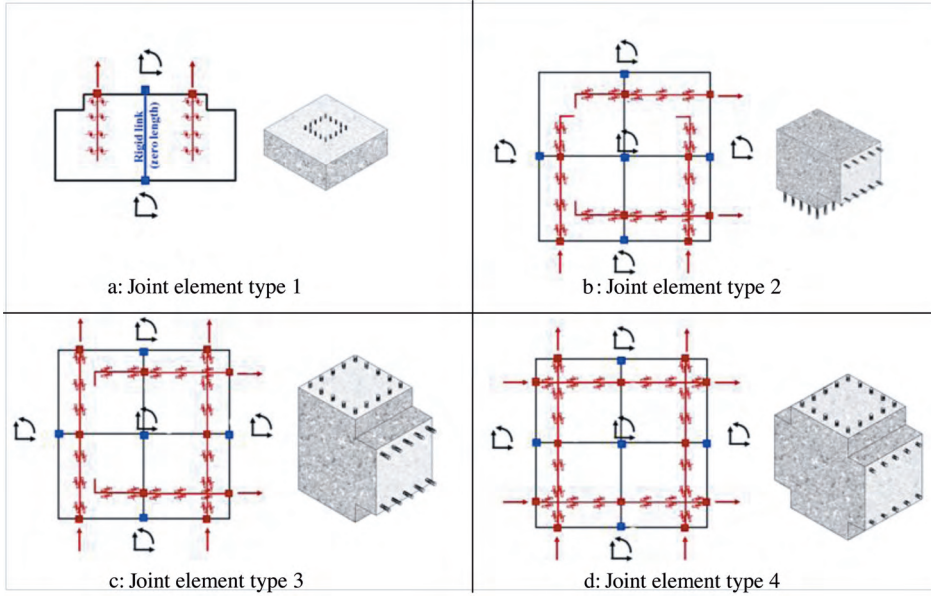


Figure 10. Types of JEs in a 2-dimensional RCF.

3. Behavior of materials

3.1. Concrete cyclic stress-strain relation

The monotonic envelope curve for confined concrete, introduced by Park et al. (1972) and later extended by Scott et al. (1982), was adopted for the compression region because of its simplicity and computational efficiency. It was also assumed that the concrete behavior is linearly elastic in the tension region before the tensile strength, and beyond that, the tensile stress decreases linearly with increasing tensile strain. The ultimate state of tension behavior is assumed to occur when the tensile strain exceeds the value given in Eq. (10).

$$\varepsilon_{ut} = 2 \times (G_f/f_t) \times \ln(3/L)/(3 - L) \quad (10)$$

Here, L denotes the element length in millimeters and G_f is the fracture energy that is dissipated in the formation of a crack of unit length per unit thickness; it is considered as a material property. f_t is the concrete tensile strength. For normal-strength concrete, the value of G_f/f_t is in the range of 0.005-0.01 (Welch and Haisman, 1969). In this research, the average value of 0.0075 is assumed for G_f/f_t . The rules suggested by Yassin (1994) were adopted for considering the hysteresis behavior of the concrete stress-strain relation in the compression and tension regions.

3.2. Cyclic stress-strain relation of steel bars

The Giuffre-Menegoto-Pinto model was adopted to represent the stress-strain relationship of steel bars. This model was initially proposed by Giuffre and Pinto (1970) and later used by Menegoto and Pinto (1973). It was modified by Filippou et al. (1983) to include isotropic strain hardening. The model agrees very well with experimental results from cyclic tests of reinforcing steel bars.

3.3. Cyclic shear stress-strain relation of joints

The adopted model to represent the shear stress-strain of joints was that proposed by Anderson et al. (2008). This model replicates cyclic degradation in strength, stiffness (modulus), and energy dissipation for unloading and reloading behavior.

3.4. Cyclic bond stress-slip relation

In the first 3 analyses, there is no need for defining the bond-slip equation, because they assume a perfect bond between the bar and concrete. In the fourth analysis, however, the bond stress-slip equation is necessary for implementation in the calculation of JEs and BCEs. Bond stress refers to the shear stress acting parallel to an embedded steel bar on the contact surface between reinforcing bars and concrete. Bond slip is defined as the relative displacement between the steel bar and the concrete. In this study, 2 models were used for the bond stress-bond slip relationships, the first for the bond-slip behavior through the length of the BCE and the second for the bond-slip behavior through the length of the RCSE and pull-out behavior of the bars in the JEs. Among several models proposed by researchers, that proposed by Eligehausen et al. (1983) was adopted for both of the specified types of behavior. In this model, the effects of many variables, such as spacing and height of lugs on the steel bar, concrete compressive strength, thickness of concrete cover, steel bar diameter, and end bar hook, were considered. More details about unloading and reloading branches and bond strength degradation related to this model are given in the work of Gan (2000).

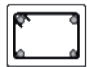
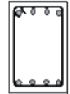
4. Numerical investigation

As the first specimen, a one-bay, one-story frame was studied under the name of specimen 1, and the analytical results were compared with the corresponding experimental results. In numerical modeling, beams and columns are subdivided into a sufficient number of BCEs. Because the formulation is displacement-based and the response depends on the element size, the length of the BCE needs to be short enough. As a simple suggestion, the length of the BCE can be selected as equal to or smaller than the average crack spacing in the beam or column. In these cases, convergence will be achieved in the numerical results. The equation given by CEB-FIP (1978) was adopted for the calculation of average crack spacing. Specimen 1 was tested by Alin and Altin (2007) and was modeled as the combination of BCEs, JE type 1, and JE type 2. Some details are shown in Table 2 and Figure 11. Columns have no constant axial load and the loading is carried out laterally only.

For nonlinear solving of this model, a Newton-Raphson method that involved controlling displacement was used. In Figure 12, experimental results are compared with analytical ones produced in analyses 1-4 in a pushover status for specimen 1. In Figure 13, the results are compared in a cyclic status. Results show that in analysis 1, where the bond-slip effect and nonlinear behavior of the joint are not included, experimental results are very different from analytical ones. This difference is high for stiffness. By inserting the equivalent bond-slip

effect in analysis 2, results become more accurate with regard to resistance but do not change much with respect to stiffness, especially the stiffness of unloading and reloading paths. In analysis 3, the analytical accuracy of calculated resistance and stiffness improves while no good agreement appears yet between the unloading and reloading paths, particularly in the final cycles. Analysis 4 makes for a considerable improvement in the results, and the analytical unloading and reloading paths are estimated with good precision. Thus, it can be said that this method enjoys a good accuracy in working out the members' resistance, stiffness, and real nonlinear behavior.

Table 2. Details of specimen 1.

	Columns	Beam
Section view		
Main bars (number × diameter)	4 × 10 mm	8 × 8 mm
Stirrups	6 mm bars @ 40 & 80 mm c/c	4 mm bars @ 40 mm c/c
Cross-section (mm)	Width: 150, depth: 100	Width: 150, depth: 300
f_C (MPa)	21.8	21.8
f_y of main bars (MPa)	475	592
f_y of stirrups (MPa)	427	326
Number of subdivisions	10	12
Type of JEs	1 and 2	

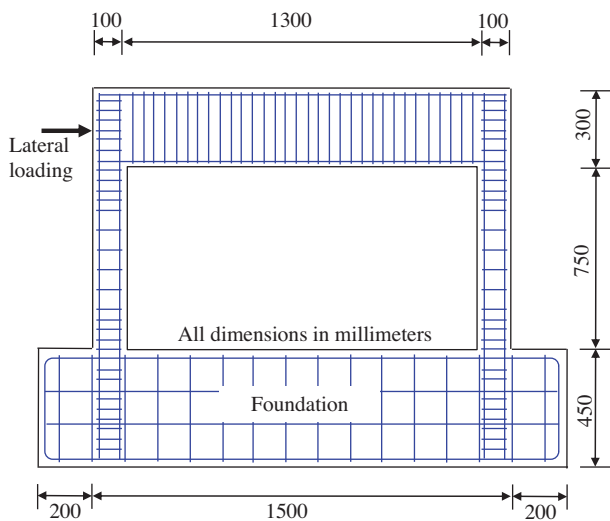


Figure 11. Geometry of specimen 1 (Alin and Altin, 2007).

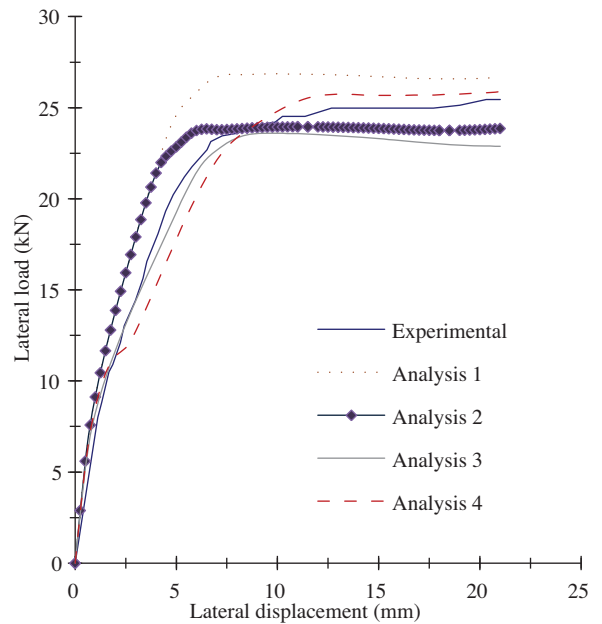


Figure 12. Experimental and analytical pushover load-displacement responses for specimen 1.

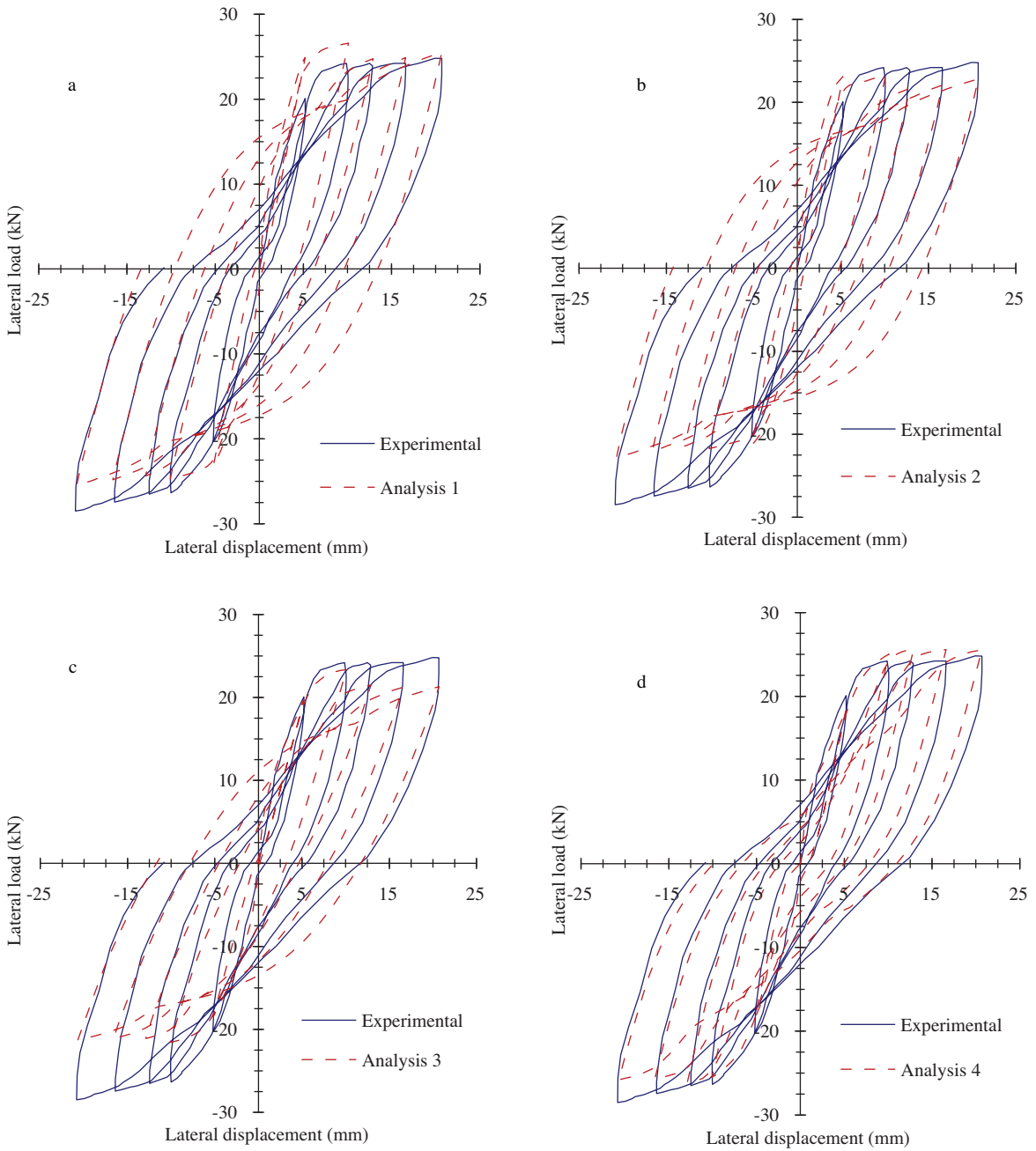


Figure 13. Experimental and analytical cyclic load-displacement responses for specimen 1.

As specimen 2, a column under lateral cyclic loading was investigated. This specimen had a constant axial load with a magnitude of 350 kN and was tested by Qiu et al (2002). Some details are shown in Table 3 and Figure 14. In numerical modeling, the specimen is modeled as the combination of 10 BCEs and type 1 of JEs. Figure 15 shows the result of analysis 4 and experimental load-displacement responses with very good similarity and precision for specimen 2. Thus, analysis 4 enjoys a good accuracy in working out the members' resistance and stiffness and during cyclic loading.

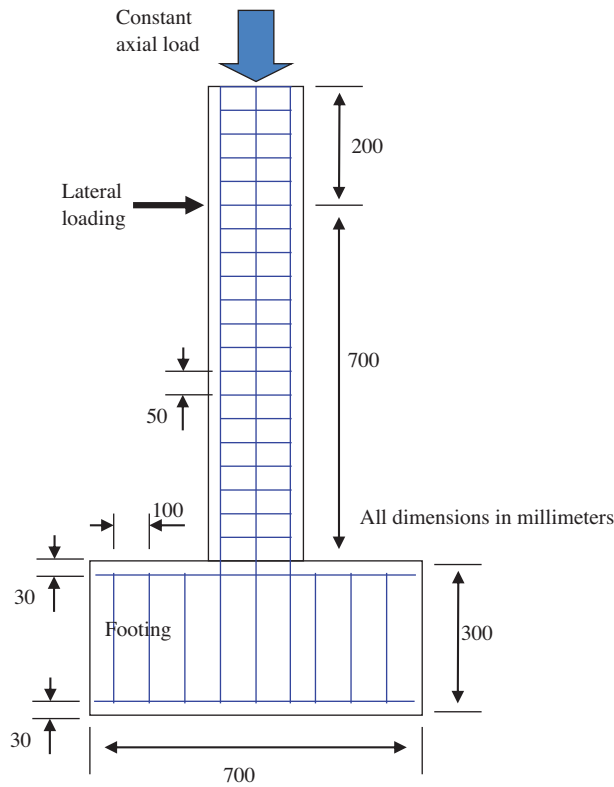


Figure 14. Geometry of specimen 2 (Qiu et al., 2002).

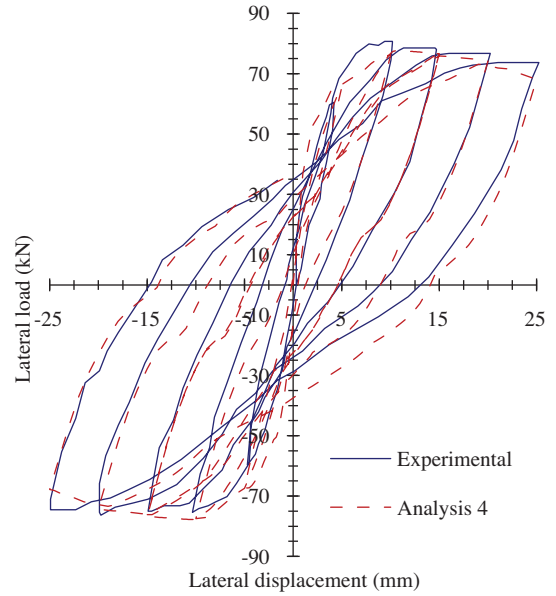
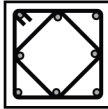


Figure 15. Experimental and analytical cyclic load-displacement responses for specimen 2.

Table 3. Details of specimen 2.

	Column
Section view	
Main bars (number × diameter)	8 × 12 mm
Stirrups	6-mm bars @ 50 mm c/c
Cross-section (mm)	Width: 200, depth: 200
f_c (MPa)	40
f_y of main bars (MPa)	460
f_y of stirrups (MPa)	420
Number of subdivisions	10
Type of JE	1

In addition, due to the capabilities of nonlinear modeling of the JE, using analysis 4 and directly implementing the bond-slip effect in calculations, we can study the analytical behavior of elements resulting from a decreased embedded length or reduction of the bond-slip effect in longitudinal bars. In Figure 16a, the analytical results of specimen 1 are provided, assuming that the columns' longitudinal bars are constrained 5

cm in the foundation. It should be added that, in the tested main model, the columns' longitudinal bars were continued 45 cm into the foundation and were not pulled out. Results reveal that by reducing the embedded length at the foot of a column, bars are increasingly pulled out of the foundation and, consequently, the lateral capacity of the frame will be lessened. Figure 16b presents a comparison of real experimental results with analytical ones for specimen 1, assuming that the bar-concrete bond-slip effect around the joint and the BCEs is weakened. The stress bond-slip relationship has been considered as linear with a slope of 5 MPa/mm. This slope signals a weak bond. According to the results, due to insufficiency of the bond between the concrete and bars, the stiffness of the RC elements decreases. This result is also revealed in the unloading and reloading paths.

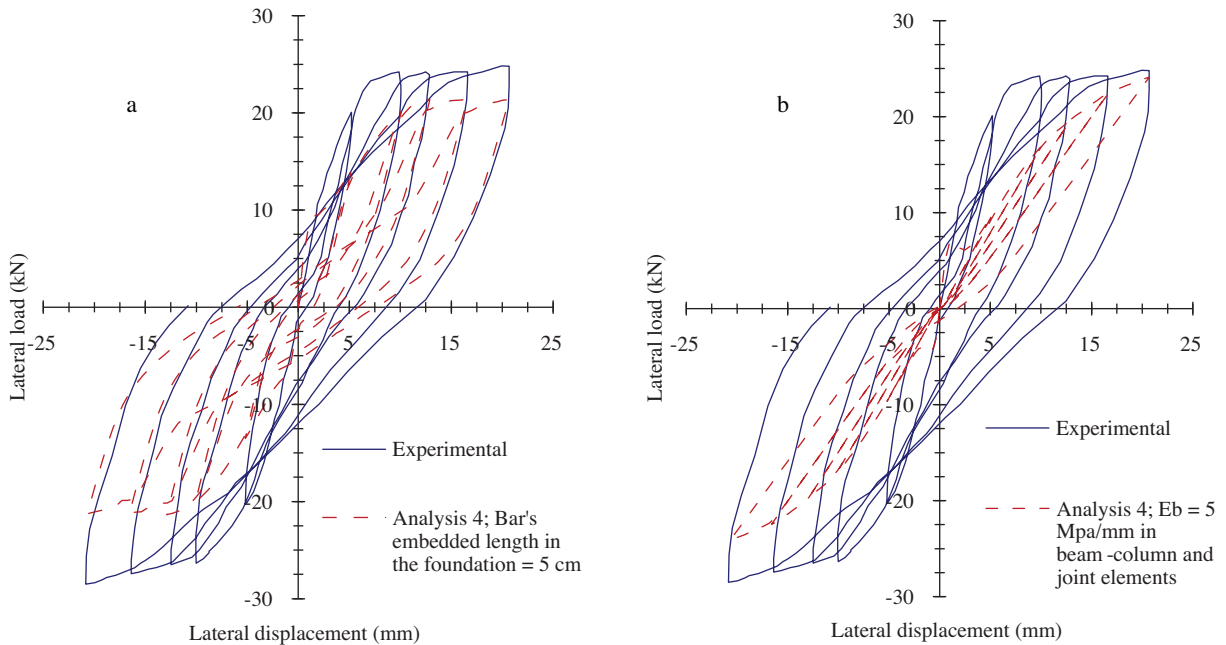


Figure 16. Effect of bar's pull-out and weak bond strength on load-displacement responses of specimen 1.

5. Conclusion

According to the results, the presence or absence of the bond effect in numerical modeling and analysis will bring about considerably different results, including results for deformation and forces. When the bond-slip effect is excluded, the values for the stiffness of the elements and for internal forces appear to be higher than their real figures. Consequently, the values obtained for deformation and energy waste in the hysteresis circuits tend to be lower than the real values. All of the studied methods for inserting the bond-slip effect into the fiber model can relatively improve the accuracy of analytical results compared to experimental ones. The proposed method of this study has proved to enjoy the highest accuracy with regard to cyclic analysis. Among the features of the proposed method, we refer to its ability for modeling beam-column and JE nonlinear behavior separately. In addition, depending on the location of the JE in the RCF and its governing behavior feature, various types of joints can be utilized. Although compared to other studied methods the suggested method involves more numeric calculations and higher degrees of freedom in modeling, it enjoys a higher speed of modeling and less need for calculations compared to methods such as finite element modeling, implementing the bond-slip effect using contact (or link) elements. Moreover, the proposed method can be used in analyses that require high

accuracy. In conclusion, the authors of this paper suggest that this method will be useful and remarkably accurate for the nonlinear cyclic analysis of RCMRF.

References

- Alath, S. and Kunnath, S.K. "Modeling Inelastic Shear Deformation in RC Beam-Column Joints", Engineering Mechanics: Proceedings of 10th Conference, University of Colorado at Boulder, Boulder, Colorado, Vol. 2. New York, ASCE, 822-825, 1995.
- Alin, Ö. and Altin, S. "An Experimental Study on Reinforced Concrete Partially Infilled Frames", Engineering Structures, 29, 449-460, 2007.
- Anderson, M., Lehman, D. and Stanton, J. "A Cyclic Shear Stress-Strain Model for Joints without Transverse Reinforcement", Engineering Structures, 30, 941-954, 2008.
- Belarbi, A. and Hsu, T.T.C. "Constitutive Laws of Concrete in Tension and Reinforcing Bars Stiffened by Concrete", ACI Structural Journal, 91, 465-474, 1994.
- Biddah, A. and Ghobarah, A. "Modeling of Shear Deformation and Bond Slip in Reinforced Concrete Joints", Structural Engineering Mechanics, 7, 413-432, 1999.
- Brancaleoni, F., Ciampi, V. and Di Antonio, R. "Rate-Type Models for Nonlinear Hysteretic Structural Behavior", EUROMECH Colloquium, Palermo, Italy, 1983.
- Clough, R.W., Benuska, K.L. and Wilson, E.L. "Inelastic Earthquake Response of Tall Buildings", Proceedings of Third World Conference on Earthquake Engineering, 2, 68-89, New Zealand, 1965.
- Comite Euro International du Beton. "CEB-FIP Model Code for Concrete Structures", Paris, 1978.
- Eligehausen, R., Popov, E. and Bertero, V. "Local Bond Stress-Slip Relationship of Deformed Bars under Generalized Excitations", Report No. UCB/EERC-83/23, Earthquake Engineering Center, University of California, Berkeley, 1983.
- Elmorsi, M., Kianoush, M.R. and Tso, W.K. "Modeling Bond-Slip Deformations in Reinforced Concrete Beam-Column", Canadian Journal of Civil Engineering, 27, 490-505, 2000.
- Filippou, F.C., D'Ambrisi, A. and Issa, A. "Nonlinear Static and Dynamic Analysis of Reinforced Concrete Subassemblages", Report No. UCB/EERC-92/08, Earthquake Engineering Research Center, College of Engineering, University of California, Berkeley, 1992.
- Flippou, F.C., Popov, E. and Bertero, V. "Effect of Bond Deterioration on Hysteretic Behavior of Reinforced Concrete Joints", Report No. EERC 83-19, Earthquake Engineering Research Center, University of California, Berkeley, 1983.
- Gan, Y. "Bond Stress and Slip Modeling in Nonlinear Finite Element Analysis of Reinforced Concrete Structures", MSc Thesis, Department of Civil Engineering, University of Toronto, 2000.
- Giuffrè, A. and Pinto, P.E. "Il Comportamento del Cemento Armato per Sollecitazioni Cicliche di forte Intensità", Giornale del Genio Civile, Maggio, Italy, 1970.
- Hashemi, S.Sh., Tasnimi A., Soltani M., "Nonlinear Cyclic Analysis of Reinforced Concrete Frames, Utilizing New Joint Element", Scientia Iranica Journal, 16, 490-501, 2009.
- Kwak, H.G. and Kim, J.K. "Implementation of Bond-Slip Effect in Analyses of RC Frames under Cyclic Loads Using Layered Section Method", Engineering Structures, 28, 1715-1727, 2006.
- Kwak, H.G. and Song, J.Y. "Cracking Analysis of RC Members Using Polynomial Strain Distribution Function", Journal of Engineering Structures, 24, 455-488, 2006.
- Lee, J.Y., Kim, J.Y. and Oh, G.J. "Strength Deterioration of Reinforced Concrete Beam-Column Joints Subjected to Cyclic Loading", Engineering Structures, 31, 2070-2085, 2009.

- Limkatanyu, S. "Reinforced Concrete Models with Bond-Interfaces for the Nonlinear Static and Dynamic Analysis of Reinforced Concrete Frame Structures", PhD Thesis, Department of Civil Engineering, University of Colorado, 2002.
- Limkatanyu, S. and Spacone, E. "Reinforced Concrete Frame Element with Bond Interfaces. Part I: Displacement-Based, Force-Based, and Mixed Formulations", *Journal of Structural Engineering*, ASCE, 128, 346- 355, 2002a.
- Limkatanyu, S. and Spacone, E. "Reinforced Concrete Frame Element with Bond Interfaces. Part II: State Determinations and Numerical Validation", *Journal of Structural Engineering*, ASCE, 128, 356-364, 2002b.
- Lowes, L.N., Mitra, N. and Altoontash, A. "A Beam-Column Joint Model for Simulating the Earthquake Response of Reinforced Concrete Frames", Report No. 2003/10, Pacific Earthquake Engineering Research Center (PEER), 2004.
- MathWorks, "MATLAB, the Language of Technical Computing", Version 7.6.0. (R2008a), 2008.
- Mazars, J., Kotronis, P., Ragueneau, F. and Casaux, G. "Using Multifiber Beams to Account for Shear and Torsion Applications to Concrete Structural Elements", *Computer Methods in Applied Mechanics and Engineering*, 195, 7264-7281, 2006.
- Menegoto, M. and Pinto, P. "Method of Analysis for Cyclically Loaded RC Plane Frames Including Changes in Geometry and Non-Elastic Behavior of Elements under Combined Normal Force and Bending", *Symp. Resistance and Ultimate Deformability of Structures Acted on by Well-Defined Repeated Loads*, IABSE Reports, Vol. 13, Lisbon, 1973.
- Otani, S. "Inelastic Analysis of RC Frame Structures", *Journal of the Structural Division*, ASCE, 100 (ST7), 1433-1449, 1974.
- Park, R., Kent, D.C. and Sampton, R.A. "Reinforced Concrete Members with Cyclic Loading", *Journal of the Structural Division*, ASCE, 98, 1341-1360, 1972.
- Piyasena, R., "Crack Spacing, Crack Width and Tension Stiffening Effect in Reinforced Concrete Beams and One-Way Slabs", PhD Thesis, School of Engineering, Faculty of Engineering and Information Technology, Griffith University, 2002.
- Qiu, F., Li, W., Pan, P. and Qian, J. "Experimental Tests on Reinforced Concrete Columns under Biaxial Quasi-Static Loading", *Engineering Structures*, 24, 419-428, 2002.
- Scott, B.D., Park, R. and Priestley, M.J.N. "Stress-Strain Behavior of Concrete Confined by Overlapping Hoops at Low and High Strain Rates", *ACI Journal*, 79, 13-27, 1982.
- Soleimani, D., Popov, E.P. and Bertero, V.V. "Nonlinear Beam Model for R/C Frame Analysis", 7th ASCE Conference on Electronic Computation, St. Louis, 1979.
- Spacone, E., Filippou, F.C. and Taucer, F.F. "Fibre Beam-Column Model for Nonlinear Analysis of R/C Frames: Part I. Formulation", *Earthquake Engineering and Structural Dynamics*, 25, 711-725, 1996.
- Welch, G.B. and Haisman, B. "Fracture Toughness Measurements of Concrete", Report No. R42, Sydney, University of New South Wales, 1969.
- Yassin, M.H.M. "Nonlinear Analysis of Pre-Stressed Concrete Structures under Monotonic and Cyclic Loads", PhD Thesis, University of California, Berkeley, 1994.